April 2001 • NREL/CP-610-30848

Conference Paper

Roof Integrated Solar Absorbers: The Measured Performance of "Invisible" Solar Collectors

Preprint

C.J. Colon
Florida Solar Energy Center

T. Merrigan
National Renewable Energy Laboratory

To be presented at the Solar Forum 2001
Washington, D.C.
April 21–25, 2001

National Renewable Energy Laboratory

1617 Cole Boulevard
Golden, Colorado 80401-3393

NREL is a U.S. Department of Energy Laboratory
Operated by Midwest Research Institute • Battelle • Bechtel

Contract No. DE-AC36-99-GO10337

Available electronically at http://www.osti.gov/bridge

Available for a processing fee to U.S. Department of Energy
and its contractors, in paper, from:
U.S. Department of Energy
Office of Scientific and Technical Information
P.O. Box 62
Oak Ridge, TN 37831-0062
phone: 865.576.8401
fax: 865.576.5728
email: reports@adonis.osti.gov

Available for sale to the public, in paper, from:
U.S. Department of Commerce
National Technical Information Service
5285 Port Royal Road
Springfield, VA 22161
phone: 800.553.6847
fax: 703.605.6900
email: orders@ntis.fedworld.gov
online ordering: http://www.ntis.gov/ordering.htm

Printed on paper containing at least 50% wastepaper, including 20% postconsumer waste

ROOF INTEGRATED SOLAR ABSORBERS: THE MEASURED PERFORMANCE OF "INVISIBLE" SOLAR COLLECTORS

Carlos J. Colon
Florida Solar Energy Center
University of Central Florida
1679 Clearlake Road
Cocoa, Florida, 32922
(321) 638 -1435
carlos@fsec.ucf.edu

Tim Merrigan
National Renewable Energy Laboratory
1617 Cole Boulevard
Golden, Colorado, 80401
(303) 384 - 7349
tim_merrigan@nrel.gov

ABSTRACT

The Florida Solar Energy Center (FSEC), with the support of the National Renewable Energy Laboratory (NREL), has investigated the thermal performance of solar absorbers which are an integral yet indistinguishable part of a building's roof. The first roof-integrated solar absorber (RISA) system was retrofitted into FSEC'S Flexible Roof Facility in Cocoa, Florida in September 1998. This "proof-of-concept" system uses the asphalt shingle roof surface and the plywood decking under the shingles as an unglazed solar absorber. The absorbed solar heat is then transferred to water that is circulated from a storage tank through polymer tubing attached to the underside of the roof decking. Data collected on this direct 3.9 m^2 (42 ft^2) solar system for a period of 12 months indicates that it was able to provide an average of 3.4 kWh per day of hot water energy to the storage tank under a 242 liters (64 gal) per day load. The RISA system's average annual solar conversion efficiency was also determined to be 8 percent, with daily efficiencies reaching a maximum of 13 percent. In addition, a thermal performance equation has been determined to characterize the Phase 1 RISA system's year-long efficiency under various ambient temperature, insolation, and wind speed conditions.

As a follow-on to the proof-of-concept phase, two prototypes of approximately 4.5 m^2 (48 ft^2) surface area were constructed and submitted for FSEC thermal performance testing. These Phase 2 RISA prototypes differ in both roof construction and the position of the polymer tubing. One prototype is similar to the "proof-of-concept" RISA system as it employs an asphalt shingle roof surface and has the tubing mounted on the underside of the plywood decking. The second RISA prototype uses metal roofing panels over a plywood substrate and places the polymer tubing between the plywood decking and the metal roofing. Both prototypes were tested according to ASHRAE Standard 93 for determining the thermal performance of solar collectors. From performance data measured both outdoors and indoors using a solar simulator, $F_R(\tau\alpha_e)$'s were determined to be approximately 18% and 33% for the asphalt shingle and metal roof RISA prototypes, respectively. In addition, the coefficients of linear and second-order efficiency equations were also determined at various wind speeds. Finally, an FSEC thermal performance rating was calculated at the low and intermediate temperature levels. In summary, this paper is a first look at the thermal performance results for these "invisible" solar absorbers that use the actual roof surface of a building for solar heat collection.

NOMENCLATURE

A_r = absorber area of collector, m^2 (ft^2)
F_R = solar collector heat removal factor, dimensionless
Gt = global solar irradiance incident upon the aperture plane of collector, W/m2 (Btu/h • ft^2)
t_c = collector temperature (average of the fluid inlet and outlet temperature,°C (°F)
$t_{f,e}$ = temperature of the transfer fluid leaving the collector, °C (°F)
$t_{f,e,initial}$ = temperature leaving collector at the beginning of time constant period, °C (°F)
$t_{f,e,T}$ = temperature of the heat transfer fluid leaving the collector at specified time, °C (°F)
$t_{f,i}$ = temperature of the transfer fluid entering the collector, °C (°F)
α = absorptance of the collector absorber surface for solar radiation, dimensionless
η = collector efficiency (actual useful energy collected divided by solar energy intercepted by absorber area)
τ = transmittance of the solar collector cover plate, dimensionless
U_L = solar collector heat transfer loss coefficient W/(m^2 • °C) (Btu/(h • ft^2 •°F))
$(\tau\alpha)_e$ = effective transmittance-absorptance product, dimensionless

INTRODUCTION

As part of the "New Concepts for Solar Thermal Systems" project that was begun by the National Renewable Energy Laboratory (NREL) in 1997 for the U.S. Department of Energy's Solar Buildings Program, the Florida Solar Energy Center (FSEC) conducted a Phase 1 experimental investigation to determine the proof-of-concept of a roof-integrated solar absorber. (Merrigan et al., 1997) An asphalt shingle roof section on FSEC's Flexible Roof Facility in Cocoa, Florida was used to install a solar absorber system that was completely underneath the roof surface. Installation of this absorber in 1998 was performed by attaching aluminum heat transfer tracks 10.2 cm (4 in) wide by 122 cm (48 in) long to the underside of the plywood roof deck. The aluminum tracks are a commercially-available product that are typically used for installing radiant floor heating systems underneath wood floors. A perspective view of the placement of the tracks in the roof of the building can be seen in Fig. 1. Three rows of aluminum tracks were installed

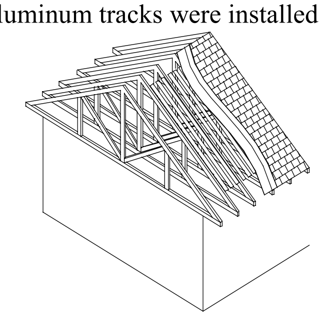

Figure 1: Perspective view of the "proof-of-concept" Roof Integrated Solar Absorber (RISA) installed between trusses.

between each pair of roof trusses (as also indicated in the top part of Figure 4.) Because of the space between the tracks and the width of the trusses themselves, the actual absorber contact area was approximately 48 percent of the roof's 8.2 m^2 (88 ft^2) surface area. The asphalt shingle roof itself had a pitch of 22.6 degrees from the horizontal and faced south. Twelve millimeter (½ in) nominal cross-linked polyethylene (PEX) tubing with an oxygen barrier of aluminum (PEX-AL-PEX) was snapped into the heat transfer plates from inside the attic space. The polymer tubing is therefore protected from the weather, especially ultraviolet radiation, and does not affect the aesthetic appearance of the roof itself. Underneath the 45 m (147 ft) of continuous tubing, 1.9 cm (0.75 in) rigid foam insulation with an aluminum foil surface (R=4.3) was installed to minimize both convective and radiative heat transfer into the attic. The inlet and outlet of the tubing were connected to a nominal 300 liter (80 gallon) solar storage tank and 1/40 horsepower circulation pump. The pump was controlled by a standard differential controller as in a typical Florida direct solar water heating system, where pressurized water in the storage tank is directly circulated through the absorber tubing. The PEX-AL-PEX tubing is rated at 200 psi at 23°C (73 F) and at 125 psi at 82°C (180 F). (Plastic Pipe Institute, 1999) Its wall thickness is 2.0 mm (0.08 in) and coefficient of thermal conductivity is 0.45 W/m•°C (3.12 Btu/h/ft^2/in/°F).

The "proof-of-concept" RISA system was instrumented to determine its thermal performance and solar conversion efficiencies. The system has been operating and data has been collected since December 1998. Figure 2 displays twelve months of hourly thermal performance data from January to December 1999. The data is presented in the form of a collector efficiency plot for all hours when the solar insolation was greater than 790 Watts/m^2 and for all wind speeds. A linear regression of more than 750 data points is also indicated in Fig. 2 with a y-axis intercept of 17.9% and a slope of -461.1 °C/W/m^2.

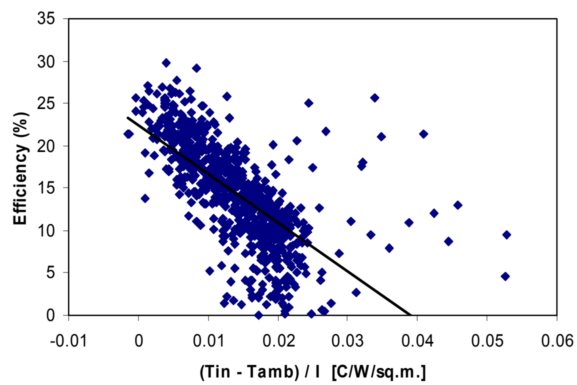

Figure 2: Efficiency of "proof-of-concept" RISA system from January 1, 1999 to December 31, 1999.

The absorber area used in the calculation of the efficiency in Figure 2 was 4.9 m^2 or 60 percent of the roof's 8.2 m^2 surface area, since it was estimated that 25 percent of the roof area not in contact with the aluminum heat transfer tracks was still providing heat to the water in the tubing. (Burch, 2000) As will be seen in the thermal performance test results of the Phase 2 RISA prototypes, this estimate of the edge effects of the heat transfer tracks was fairly accurate.

On August 23, 1999, the system was modified to automatically purge 64 gallons of hot water during three intervals (morning, noon, and late afternoon) on a daily basis. Table 1 is a summary of the thermal performance of this system during a one-year period from October 1999 to September 2000. The monthly table shows the average daily amount of energy delivered to the storage tank by the solar absorber in Btus and kilowatt-hours (kWh). The table also includes the average daily hot water energy used and gallons purged from the storage tank. The last column in Table 1 indicates the roof-integrated absorber's

Table 1: One-year summary of the "proof-of-concept" RISA system in Cocoa, Florida

Month of Year	Delivered Energy (kWh/day)	Delivered Energy (Btu/day)	Energy Used (kWh/day)	Energy Used (Btu/day)	Hot Water Used (liters/day)	Hot Water Used (gal./day)	Solar Conversion Efficiency (%)
Oct '99	3.0	10,411	2.64	9,022	241	63.6	7.59
Nov '99	3.1	10,644	2.77	9,466	246	64.9	7.87
Dec '00	2.7	9,081	2.30	7,843	246	64.9	7.51
Jan '00	3.2	10,878	2.72	9,290	246	64.9	8.01
Feb '00	3.7	12,604	3.00	10,274	246	64.9	7.91
Mar '00	4.0	13,829	3.39	11,565	245	64.8	8.10
Apr '00	3.9	13,310	3.26	11,127	246	64.9	7.02
May '00	4.4	15,045	3.43	11,707	246	64.9	8.05
Jun '00	3.9	13,143	2.94	10,050	238	64.8	8.32
Jul '00	4.3	14,576	2.94	10,053	233	61.5	9.20
Aug '00	4.0	13,529	3.39	11,596	253	66.8	8.71
Sep '00	3.8	13,103	2.90	9,903	245	64.8	8.41
Average 10/99-9/00	3.4	11,530	2.97	10,158	2443	64.4	8.06

conversion efficiency (delivered energy / incident solar energy) expressed as a percentage. The last row on the table indicates the average performance during the one-year period.

PHASE 2 ROOF-INTEGRATED SOLAR ABSORBER (RISA) DESIGNS

Phase 2 of the "New Concepts for Solar Thermal Systems" project was begun in November 1999. (Merrigan et al., 1999) One of the primary objectives of Phase 2 was to construct two RISA prototypes that could be tested in a standard collector performance test. One prototype was again made with an asphalt shingle roof surface and a new prototype was constructed with a metal roof surface.

ASPHALT SHINGLE RISA PROTOTYPE

As in Phase 1, construction of the Phase 2 asphalt shingle RISA prototype was also based on an "underneath-the-roof" design. The roof itself consisted of nominal 12 cm (½ in) thick plywood nailed over a wooden frame that was 1.2 m (4 ft) wide and 3.6 m (12 ft) long with two truss bays that had a typical on-center (o.c.) spacing of 61 cm (24 in), as depicted in Fig. 3. Exterior grade (CDX) plywood typically used for roof sheathing was the roof deck substrate. Just as in the Phase 1 design, 12 mm (½ in) PEX-AL-PEX tubing with a 16 mm outside diameter was used for the absorber piping. A total of 31 meters (102 ft) of PEX tubing was routed in a series configuration with four rows of PEX tubing within each bay of the prototype. The whole assembly was insulated underneath with 2.5 cm (1 in.) rigid insulation with a nominal insulation value of R=5.4. The prototype's roof surface consisted of a three-tab "Weathered Gray" asphalt shingle (GAF Sentinel) with

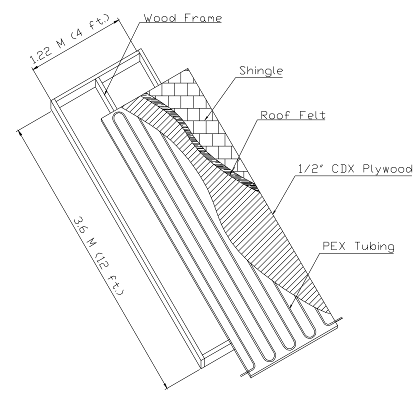

Figure 3: Layers of the asphalt shingle RISA prototype.

an estimated solar absorptance of approximately 91.8%. (Parker et al., 1993) The shingles were installed over a layer of 15-lb. roofing felt paper that was attached to the plywood sheathing. On the underside of the plywood sheathing, this new prototype used 0.33 mm (0.13 in) thick aluminum heat transfer plates that had four preformed ridges six inches apart (o.c.). The plates were designed to hold tubing with a nominal outside diameter of 16 mm (0.625 in). In addition, a silicon compound was applied to the tubing groove to enhance heat transfer between the plate and the tubing. The plates were attached to the plywood with 9 mm (3/8 in) screws. The differences between the original "proof-of-concept" design and the Phase 2 prototype can be observed in Fig. 4. The Phase 2 prototype had 100 percent of the plywood between the trusses that were in contact with the aluminum heat transfer plates. In addition, the plates also contained four rows of PEX tubing.

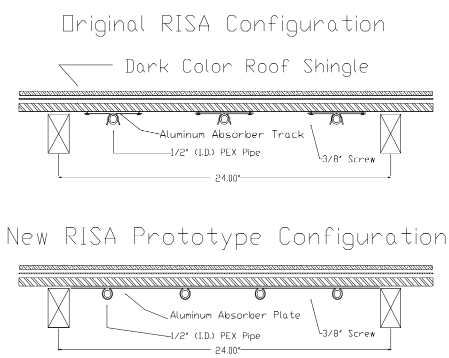

Figure 4: Cross-sectional view of both the original and Phase 2 asphalt shingle RISA prototypes.

METAL ROOF RISA PROTOTYPE

Using a similar wood truss and plywood roof decking as in the asphalt shingle prototype, a metal roof surface RISA was also constructed (Figure 5). However, in this case, the aluminum heat transfer plates were used as the prototype's roofing surface.

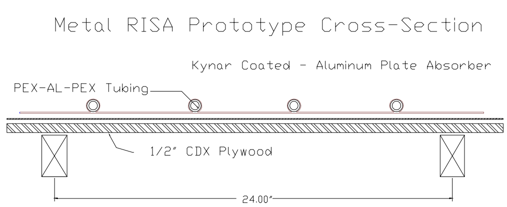

Figure 5: Cross-sectional view of the Phase 2 metal RISA prototype.

The 0.19 m^2 (2 ft^2) aluminum plates were coated with a layer of Kynar®500, which is commonly used in the metal roofing industry as a coating for steel roofing panels. (NRCA, 1996) Kynar is composed of fluoropolymers chemically known as polyvinylidene fluoride (PVF). (Raman et al., 2000) In order to determine the solar absorptance of Kynar, twelve metal roof samples of various Kynar colors were sent to an independent laboratory and tested for hemispherical spectral reflectance. (Colon, 1999) Table 2 shows some of the properties of the polymer coating applied by the regional distributor of Kynar onto the prototype's aluminum absorber plates. (Sunderman, 2000)

Table 2: Metal absorber coating specifications.

Color	Solar Absorptance	Kynar Layer (um)	Process
Hartford Green	91.5%	22.9-27.9	Sprayed and Baked 204 °C

THERMAL PERFORMANCE TESTING

The collector testing site at the Florida Solar Energy Center is located at 28.4° N. Latitude and 80.8° W. Longitude. Both indoor and outdoor collector testing is conducted using a moveable cart known as a Mobile Tracking Platform (MTP). Each MTP provides independent, two-axis tracking of the sun, with an azimuth range of ±135 degrees from south and an elevation range from 0 to 90 degrees from horizontal, with an accuracy of ±0.1 degrees under wind conditions up to 25 mph. An MTP can hold a collector or absorber structure up to 1.22 meters (4 ft) wide by 3.6 meters (12 ft) in length with a maximum load weighing up to 136 Kg (300 lbs).

Inlet water temperature and flow control were provided by a separate utility cart with an onboard chiller, heater, and variable speed pump. A regulated variable current-voltage power supply controlled the pump and the flow rate. Fluid measurement was accomplished by a high-precision turbine flow meter with an accuracy of ±1 percent. A wind velocity sensor (anemometer) was attached to the utility cart, measuring wind at a height of 2.1 meters (7 ft) from the ground. Solar irradiance was measured by an Eppley Laboratory Precision Spectral Pyranometer (PSP). The pyranometer was mounted on the MTP in the plane of the collector. Data acquisition was performed using a Campbell Scientific CR10 data logger also mounted on board the MTP. Inlet and outlet water temperatures were measured using two pairs of type-T thermocouples in differential mode. (The thermocouples were calibrated and matched in pairs to minimize error and increase accuracy.) Each pair of sensors were located to take temperature measurements before and after a fluid mixing assembly. The mixing assemblies were placed at the inlet and outlet ports of the absorber prototypes.

In addition to its well-known outdoor testing capabilities, FSEC's high bay laboratory is now equipped with a large-area solar simulator. The simulator's lamp can irradiate a surface area of 1.2 m (4 ft) by 3.6 m (12 ft), with an adjustable range up to 1500W/m^2. (Tiedemann and Maytrott, 1997) An indoor fan capable of moving 2,265 cubic meters/s (80,000 cfm) of air can simulate wind conditions with its variable speed control capabilities.

Thermal performance testing was conducted according to American Society of Heating, Refrigerating, and Air-Conditioning Engineers (ASHRAE) Standard 93-

1986 guidelines. (ASHRAE, 1991) Physically, the roof-integrated solar absorbers described here are unglazed systems and would appear to be required to be tested according to ASHRAE Standard 96-1980. (ASHRAE, 1987) However, since the application currently being considered for these absorbers is the heating of potable water, ASHRAE Standard 93 was used because it requires a more typical flow rate through the collector. Table 3 lists the flow rate and wind speed requirements of both ASHRAE standards for testing glazed and unglazed collectors.

Table 3: Testing criteria for solar collectors.

ASHRAE Standard	Flow Rate	Wind Conditions
93-86 (glazed)	0.02 kg/s •m^2	3.5-4.5 m/s
96-80 (unglazed)	0.07 kg/s • m^2	<1.3 m/s

DETERMINATION OF TIME CONSTANT

A time constant for a solar collector is defined as the time required for the fluid in the solar collector to reach 63.2% of its steady state value following a step change in solar irradiance. ASHRAE Standard 93 requires that outdoor steady-state testing be conducted for a minimum period of two time constants or 10 minutes, whichever is greater. During the first attempt to determine the time constant on the asphalt shingle RISA prototype outdoors, the time constant exceeded a period of 30 minutes. These results were mainly attributed to the amount of thermal mass within the roof deck structure. Further efforts to determine the time constant outdoors were complicated by the requirement of maintaining the inlet water temperature within a degree of the outdoor air temperature. A sudden outdoor temperature rise or fall could have an effect on the time constant results, especially when testing exceeds a time period of 30 minutes. Because of the dynamic outdoor temperature and wind conditions, all succeeding time constant tests were performed indoors with the solar simulator.

At least two time constant tests were performed on each of the prototypes. The time constant test was performed by irradiating the prototype absorber for a period of at least 30 minutes. A cover was then placed on top of the surface. The cover was supported around its perimeter and raised to at least 10 cm (4 in) from the surface to allow cooling. The solar simulator was left operating during the cool-down period to maintain and prevent the indoor temperature from changing drastically. The test was performed with air flowing at 1.8 m/s (4 mph).

The time constant (T) was determined using the ratio of temperatures of the heat transfer fluid (water) as shown in the following formula:

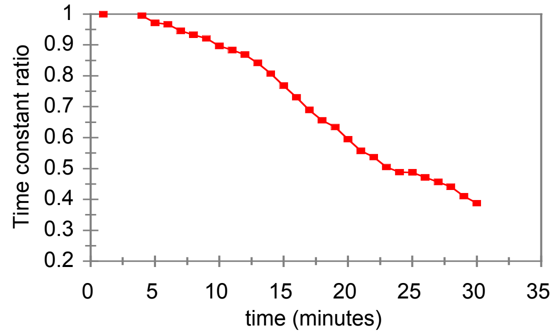

Figure 6: Time constant test for asphalt shingle RISA prototype.

$$\frac{tf,e,T - tf,i}{tf,e,initial - tf,i} \qquad (1)$$

The actual time constant T was determined by the amount of time the ratio in the above formula changes from 1.0 to 0.368. A temperature decay profile can be observed in Fig. 6 during a test performed on the asphalt shingle RISA prototype. During both tests performed, a time constant ratio of at least 1.0 was maintained for a period of three minutes before the decay was noticeable. Again this is primarily due to the thermal mass of the roof-integrated absorber. The average time constant for the shingle prototype was 29 minutes.

In turn, two tests were performed indoors on the metal roof RISA prototype to determine its time constant. The results and thermal response of the metal prototype were noticeably shorter when compared to the shingle prototype. Figure 7 plots the results of one of the tests performed on the metal roof prototype. The average time constant for the metal roof prototype was 3 minutes and 42 seconds.

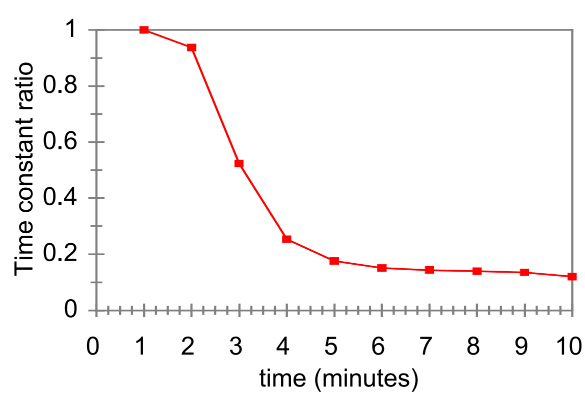

Figure 7: Time constant test for metal roof RISA prototype.

THERMAL PERFORMANCE RESULTS

Results from the thermal performance testing are presented in terms of the thermal efficiency of the solar absorber, where efficiency (η) is defined as:

$$\eta = \frac{ActualUsefulEnergyCollected}{SolarEnergyInterceptedByAbsorberArea} \quad (2)$$

A plot of the thermal performance results obtained outdoors for the asphalt shingle RISA prototype is shown in Fig. 8, where the thermal efficiency is plotted against the collector heat loss factor $(T_i - T_a)/I_t$. Linear and second-order regressions were performed on the data to determine the slope ($-F_R U_L$) and y-axis intercept ($F_R(\tau\alpha_e)$). The efficiency can then be expressed by the following equation:

$$\eta = F_R(\tau\alpha)_e - F_R U_L(\frac{Ti - Ta}{Gt}) \quad (3)$$

ASPHALT SHINGLE RISA PROTOTYPE

The asphalt shingle RISA prototype was tested both outdoors and indoors between the months of June and August 2000. For instance, Fig. 8 was generated from 5-minute data where the outdoor wind speed averaged 2.1 m/s (4.7 mph). Efficiencies shown in this plot range between 22% and 4% for inlet temperatures of 24.4°C (76 F) to 48.3°C (119 F).

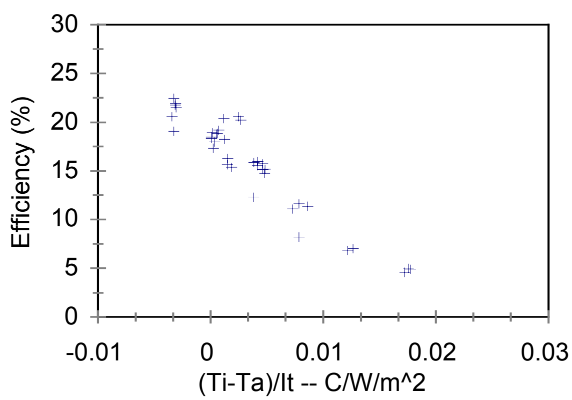

Figure 8: Outdoor thermal performance results of the asphalt shingle RISA under average wind conditions of 2.1 m/s (4.7 mph).

The y-axis intercept occurs at an efficiency of 18%, where the inlet to ambient temperature difference is zero. In a similar manner, thermal performance data for a higher outdoor wind condition of 2.9 m/s (6.6 mph) was plotted which resulted in a slight increase to the negative slope. However, the y-axis intercept remained unchanged at 18%.

The asphalt shingle RISA was then tested indoors using the solar simulator under three constant wind velocities of 0.7, 1.8 and 2.9 m/s (1.6, 4.0 and 6.9 mph). Figure 9 shows the thermal performance results of the same asphalt shingle RISA under the test conditions where air flow across the RISA was held steady at 1.8 m/s (4.0 mph) and inlet temperatures varied between 24.4°C and 48.3°C (76 F and 119 F). Minimal data scatter shows the steady thermal response under the solar simulator during the indoor testing. The y-axis intercept was found to be slightly higher at 19%. Efficiencies generated under this test varied between 22% and 8.9%, with a marked difference in the slope of the data when compared to the outdoor results at higher inlet water temperatures.

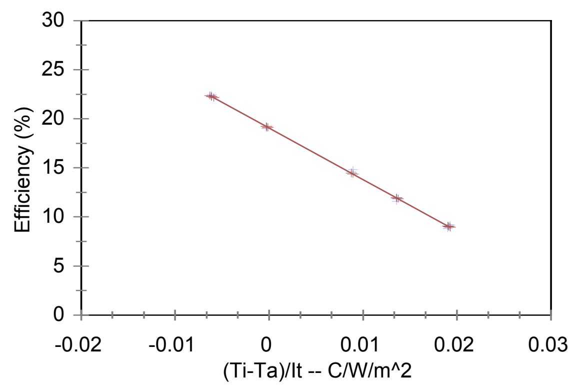

Figure 9: Indoor thermal performance results of the asphalt shingle RISA prototype under 1.8 m/s wind speed.

Table 4 summarizes all of the test results for the asphalt shingle RISA prototype under varying wind conditions outdoors as well as the controlled conditions indoors.

Table 4: Asphalt shingle prototype y-axis intercept and slope at various wind conditions.

Outdoor Testing	**3 MPH**	**5 MPH**	**7 MPH**
Y-axis intercept $F_R(\tau\alpha)$	N/A	17.8	17.7
Slope $-F_R U_L$	N/A	-810.8	-924
Indoor Testing	**3 MPH**	**5 MPH**	**7 MPH**
Y-axis intercept $F_R(\tau\alpha)$	20.7	19.1	15.5
Slope $-F_R U_L$	-464.7	-524.8	-515.5

METAL ROOF RISA PROTOTYPE

The metal roof RISA was also tested outdoors on selected days between August through October 2000. However, unlike the test period for the asphalt shingle RISA, weather conditions allowed data measurements under outdoor winds of 1.3 m/s (3 mph) or less. The results of this outdoor testing are shown in Fig. 10.

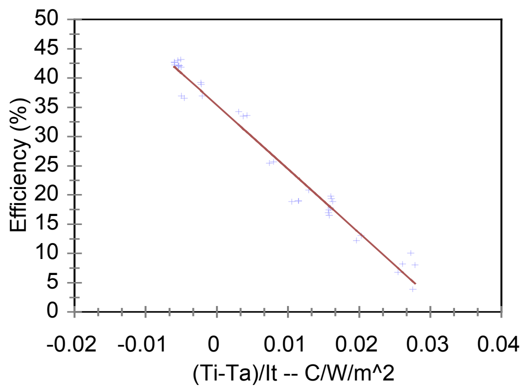

Figure 10: Outdoor thermal performance results of metal roof RISA prototype under wind conditions of 1.3 m/s (3 mph).

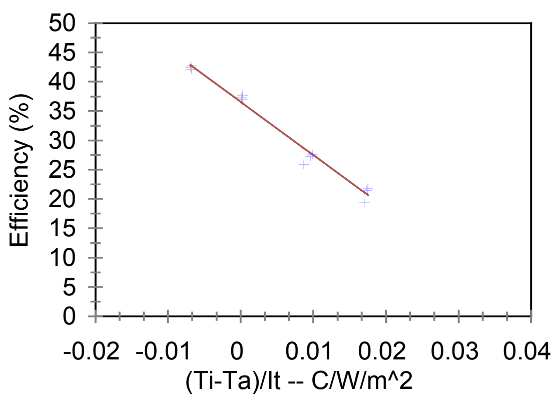

Figure 11: Indoor thermal performance results of metal roof RISA prototype under wind conditions of 1.5 m/s (3.5 mph).

Efficiencies obtained range between 42% and 4% for inlet water temperatures between 25°C and 60 °C (77 F and 141 F). The y-axis intercept was determined to be 35.4%. Similar to the asphalt shingle RISA prototype, the metal roof RISA prototype was also tested indoors under the solar simulator. Testing was performed under controlled air flow rates of 1.5, 2.1 and 3.0 m/s (3.5, 4.8 and 6.7mph). Figure 11 displays the results of the testing at a wind speed of 1.5 m/s (3.5 mph). As seen in Table 5, the results show the expected reduction in the y-axis intercept with values of 37%, 34% and 32% for increased wind conditions.

Table 5: Metal roof prototype y-axis and slope at various wind conditions.

Outdoor Testing	**3 MPH**	**5 MPH**	**7 MPH**
Y-axis intercept $F_R(\tau\alpha)$	35.4	31.2	N/A
Slope - $F_R U_L$	-1094.3	-1059.3	N/A
Indoor Testing	**3 MPH**	**5 MPH**	**7 MPH**
Y-axis intercept $F_R(\tau\alpha)$	36.6	34.0	31.8
Slope - $F_R U_L$	-906.7	-953.7	-1031.4

THERMAL PERFORMANCE RATING

In order to compare the performance of the prototype RISAs with conventional glazed and unglazed collectors, an FSEC thermal performance rating was calculated for each RISA prototype. This standard rating procedure uses the second-order efficiency curve and is based on the average collector temperature t_c, where t_c is the average of the inlet and outlet fluid temperature.

$$t_c = \frac{t_{f,i} + t_{f,e}}{2} \quad (4)$$

The collector heat loss factor is then defined by

$$LossFactor = \frac{Tc - Ta}{Gt} \quad (5)$$

The FSEC rating is based on a standard Florida day with a total solar insolation of 5,045 Watt-hours/m^2 (1,600 Btu/ft^2) distributed over a 10-hour period. Daily energies generated by the RISA prototypes were then calculated at the procedure's "low" and "intermediate" inlet temperatures of 35°C (95 F) and 50°C (122 F), respectively. With the exception of a calculation of a "high" temperature rating at 100°C (212 F), this procedure is the same as FSEC's standard method for thermal performance rating. (FSEC, 1985)

Equations 6 and 7 were the second-order equations that were determined from the test results and used to calculate the thermal output of the absorbers. The RISA prototype ratings are listed in Table 6. As indicated by the

Table 6: Summary of FSEC ratings for the asphalt shingle and metal roof RISA prototypes.

	Shingle RISA				Metal RISA			
Collector Inlet Temperature	Btu/day	Btu/ft^2/day	kWh/day	kWh/m^2/day	Btu/day	Btu/ft^2/day	kWh/day	kWh/m^2/day
Low (35°C)	5788	149	1.7	0.5	14,256	368	4.2	1.2
Intermediate (50°C)	208	5.4	0.06	0.02	2,067	53.4	0.6	0.2

thermal performance results, the metal roof RISA prototype rating is higher than the rating of the asphalt shingle RISA prototype.

Asphalt shingle RISA prototype:

$$\eta = 18.7 - 899.0\left(\frac{Tc - Ta}{Gt}\right) + 3846.8\left(\frac{Tc - Ta}{Gt}\right)^2 \quad (6)$$

Metal roof RISA prototype:

$$\eta = 33.5 - 1147.2\left(\frac{Tc - Ta}{Gt}\right) + 53.5\left(\frac{Tc - Ta}{Gt}\right)^2 \quad (7)$$

CONCLUSIONS

The "proof-of-concept" of a roof-integrated solar absorber (RISA) was successfully demonstrated in Florida. (It is interesting to note that metal-polymer absorber construction is also being investigated in Europe by Bartelsen et al., (1999).) Over a year-long period, an initial RISA design showed the ability to generate approximately 0.9 kWh/m^2 on a daily basis. While this approximately 3.9 m^2 (42 ft^2) system only had a solar conversion efficiency of eight percent, it was still able to provide approximately 3.4 kWh/day to a hot water load of 244 liters per day (64.4 gals/day). For comparison, a 3.7 m^2 (40 ft^2) glazed collector typically provides about 7 kWh/day to the same load in the same location in Florida. Hence, the "proof-of-concept" RISA system was able to generate half the hot water energy of a similarly-sized glazed collector, but it was not visible on the roof!

The thermal performance testing of the Phase 2 RISA prototypes has indicated the advantages and disadvantages of placing roof-integrated solar absorbers on the outside surface of the roof decking. A y-axis intercept of 18% for the asphalt shingle RISA prototype is only just over half of the intercept for the metal roof RISA prototype under 2 m/s outdoor wind conditions. However, the asphalt shingle RISA prototype still was able to make hot water and, because of its higher time constant, it was also not as affected as the metal roof RISA by higher wind speeds. Furthermore, the thermal performance ratings show that on a standard Florida day, the asphalt shingle and metal roof RISA prototypes were able to produce small but significant amounts of energy per surface area. Despite their conservative efficiencies at high fluid inlet temperatures (compared to glazed collectors), the typical roof surface area of a house could easily overcome the efficiency shortcoming. Generally speaking, the amount of solar energy falling upon a roof of a typical home nearly equals the energy load of the building. Roof-integrated solar absorbers present an opportunity to recover this energy without having any effects on the building's aesthetic appearance.

ACKNOWLEDGMENTS

This work was conducted under a contract from the National Renewable Energy Laboratory in support of the U.S. Department of Energy's Solar Buildings Program. The cooperation of the NREL technical monitors Andrew Watt and Russ Hewett are acknowledged. In addition, the assistance of Jim Huggins, Prasanth Thupilli, Andy Pesce, Allan Garnett and Mark Thornbloom of the Florida Solar Energy Center is also appreciated. Finally, both Steve Baer of Zomeworks and Mike Tierney of Aspen Solar Systems are acknowledged for their insight into the use of flexible polymer tubing for solar systems.

REFERENCES

American Society of Heating, Refrigerating and Air-Conditioning Engineers, Standard 93-1986 (Reaffirmed 1991), "Methods of Testing to Determine the Thermal Performance of Solar Collectors," Atlanta, Georgia, 1991.

American Society of Heating, Refrigerating and Air-Conditioning Engineers, Standard 96-1980 (Reaffirmed 1987), "Methods of Testing to Determine the Thermal Performance of Unglazed Flat –Plate Liquid-type Solar Collectors," Atlanta, Georgia 1987.

Bartelsen, B. Rockendorf, G, Venneman, N. , Tepe, R, Lorenz, K and Purkarthofer, G. "Elastomer-Metal-Absorber: Development and Application", Solar Energy Vol. 67 Nos. 4-6, pp.215-226, 1999.

Burch, J., Personal Communication, NREL, Golden, Colorado (2000).

Colon, C., "New Concepts for Solar Thermal Systems: A Roof-Integrated Solar Absorber: Project Workplan," FSEC-CR-1142-99, Cocoa, Florida, December 17, 1999.

Florida Solar Energy Center, "Operation of the Collector Certification Program," FSEC-GP-6-80 January 1985.

Maytrott, C., Tiedemann, T., "Indoor Testing Using a Large Area Solar Simulator", Florida Solar Energy Center, Cocoa, FL.

Merrigan, T., Colon, C., Huggins, J., “New Concepts for Solar Thermal Systems - A Polymeric Roof Underlayment Absorber,” FSEC-PR-042-98, Cocoa, Florida, November 10, 1997.

Merrigan, T., Colon, C., Huggins, J., Gu, L., “New Concepts for Solar Thermal Systems - Phase 2: A Roof-Integrated Solar Absorber,” FSEC-PR-99-065, Cocoa, Florida, February 22, 1999.

National Roofing Contractors Association, 1996, “The Metal Roofing Manual,” NRCA Rosemont, Illinois.

Parker, D. S., McIlvaine, J.E.R., Barkaszi, S.F., and Beal, D. J., “Laboratory Testing of Reflectance Properties of Roofing Materials,” FSEC-CR-670-93, Cape Canaveral, FL., August 1993.

Plastic Pipe Institute, “Hydrostatic Design Bases and Maximum Recommended Hydrostatic Design Stresses for Thermoplastic Piping Materials,” Technical Report 4, Washington, D.C., 1999.

Raman, R., Mantell ,S., Davidson, J., Jorgensen, G., "A Review of Polymer Materials For Solar Water Heating Systems", Proceedings of Solar 2000:Solar Powers Life, Share the Energy, June 16-21, 2000, Madison, Wisconsin.

Sunderman, D., Personal Communication, BASF Corporation, Decatur, Alabama (2000).

REPORT DOCUMENTATION PAGE

Form Approved
OMB NO. 0704-0188

1. AGENCY USE ONLY (Leave blank)	2. REPORT DATE April 2001	3. REPORT TYPE AND DATES COVERED Conference paper

4. TITLE AND SUBTITLE
Roof Integrated Solar Absorbers: The Measured Performance of "Invisible" Solar Collectors

6. FUNDING NUMBERS
SH11.6001

6. AUTHOR(S)
Carlos J. Colon and Tim Merrigan

7. PERFORMING ORGANIZATION NAME(S) AND ADDRESS(ES)

8. PERFORMING ORGANIZATION REPORT NUMBER

9. SPONSORING/MONITORING AGENCY NAME(S) AND ADDRESS(ES)
National Renewable Energy Laboratory
1617 Cole Blvd.
Golden, CO 80401-3393

10. SPONSORING/MONITORING AGENCY REPORT NUMBER
NREL/CP-610-30848

11. SUPPLEMENTARY NOTES

12a. DISTRIBUTION/AVAILABILITY STATEMENT
National Technical Information Service
U.S. Department of Commerce
5285 Port Royal Road
Springfield, VA 22161

12b. DISTRIBUTION CODE

13. ABSTRACT *(Maximum 200 words)*
The Florida Solar Energy Center (FSEC), with the support of the National Renewable Energy Laboratory, has investigated the thermal performance of solar absorbers that are an integral, yet indistinguishable, part of a building's roof. The first roof-integrated solar absorber (RISA) system was retrofitted into FSEC's Flexible Roof Facility in Cocoa, Florida, in September 1998. This "proof-of-concept" system uses the asphalt shingle roof surface and the plywood decking under the shingles as an unglazed solar absorber. Data was gathered for a one-year period on the system performance. In Phase 2, two more RISA prototypes were constructed and submitted for testing. The first used the asphalt shingles on the roof surface with the tubing mounted on the underside of the plywood decking. The second prototype used metal roofing panels over a plywood substrate and placed the polymer tubing between the plywood decking and the metal roofing. This paper takes a first look at the thermal performance results for these "invisible" solar absorbers that use the actual roof surface of a building for solar heat collection.

14. SUBJECT TERMS
Solar collectors; roof-integrated solar collectors

15. NUMBER OF PAGES

16. PRICE CODE

17. SECURITY CLASSIFICATION OF REPORT	18. SECURITY CLASSIFICATION OF THIS PAGE	19. SECURITY CLASSIFICATION OF ABSTRACT	20. LIMITATION OF ABSTRACT
Unclassified	Unclassified	Unclassified	UL